The Cardiac Muscle in the Pulmonary Vein of the Rat: A Morphological and Electrophysiological Study [1]

OSLEI PAES DE ALMEIDA, GYÖRGY MIKLÓS BÖHM, MARILENE DE PAULA CARVALHO [2] AND ANTONIO PAES DE CARVALHO
Department of Pathology, Faculty of Dentistry of Piracicaba (University of Campinas), Piracicaba, State of Sao Paulo, Brazil, Department of Morphology, Faculty of Medicine of Ribeirao Preto (University of Sao Paulo), Ribeirao Preto, State of Sao Paulo, Brazil, and Institute of Biophysics, Federal University of Rio de Janeiro, Guanabara, Brazil

ABSTRACT The pulmonary veins of albino Wistar rats were studied by means of light and electron microscopy. The media of larger veins consists of cardiac muscle fibers which extend until the vessels attain about 100 μ in diameter. This coat consists of external longitudinal fibers and internal circular fibers. The vasa vasorum are well developed and the capillaries show pseudofenestrations. The numerous adrenergic and cholinergic nerve endings do not form typical motor end-plates as seen in skeletal muscles. The ultrastructure of these media muscle fibers is similar to that of rat hearts. The smooth muscle layer of larger pulmonary veins is not continuous as it is in smaller veins where it forms cushions. Comparisons of albino rats and other rodents reveal striking differences.

Action potential shape and propagation velocity (0.5–1.2 m/s) along the myocardial coat of the pulmonary vein were similar to those observed in the left atrium and so was their sensitivity to locally applied acetylcholine. The physiological direction of propagation in rat pulmonary veins is toward the lung. This finding lends support to the hypothesis of a rhythmic, valve-like action of the striated musculature of the pulmonary venous wall during the systole and a possible role in the capacitance of the pulmonary circulation.

Rauschel recognized the existence of striated muscle in the pulmonary venous wall as long ago as 1836 (cit. in Guieysse-Pellisier, '45), and several investigators subsequently published on this subject (Stiede, 1877; Favaro, '10; Granel, '21). Short historical reviews were published by Policard et al. ('59) and Karrer ('59). Despite this previous work, there is surprisingly little information about this important structural feature of pulmonary veins.

Extensions of myocardium over the pulmonary and caval veins occur in many species (Nathan and Gloobe, '70). Generally cardiac muscle in the pulmonary side is limited to the extrapulmonary segment of the veins. In some mammals, mainly rodents, there are intrapulmonary extensions of the myocardium into the smallest venules (Kramer and Marks, '65), known as "*coeur pulmonaire*" (Guieysse-Pellisier, '45). Recent histological studies have been reported by Best and Heath ('61) and Klavins ('63). The first ultrastructural observations on pulmonary veins were made by Karrer ('59, '60) and subsequently by Policard et al. ('59), Heppleston ('61) and Ludatscher ('68). All of these workers demonstrated striated, cardiac-like muscle in direct continuity with left atrial myocardium.

The functional role of cardiac-like muscle in pulmonary veins and superior and inferior venae cavae has received little attention from physiologists. Spach et al. ('72) showed that waves of electrical activity invade the thoracic veins at their junction with the atrium of man and dog for several cms at each atrial beat. Eliakim

[1] Work done in the Department of Morphology of the Faculty of Medicine of Ribeirão Preto, University of São Paulo, and Institute of Biophysics of the Federal University of Rio de Janeiro. Supported in part by the Fundação de Amparo à Pesquisa do Estado de São Paulo, grant 71/490 — médicas; by the Conselho de Pesquisas da Universidade Federal do Rio de Janeiro, by the Conselho Nacional de Pesquisas (Brasil), and by Banco Nacional de Desenvolvimento Econômico (Brasil) Contrato FUNTEC 143.

[2] Research Fellow of the Conselho Nacional de Pesquisas (Brasil).

and Aviado ('61) demonstrated that pulmonary canine veins are also provided with some sort of "tonic" contraction which might be of importance in the production of acute pulmonary edema. Physiological and pharmacological data in rat are limited to the work of MacLeod and Hunter ('67), who showed that electrically stimulated strips of pulmonary vein behave in vitro much like atrial muscle.

The present work is concerned with the structure of pulmonary veins of the rat and their possible functional role, as determined by histological, electron microscopic and electrophysiologic techniques.

MATERIALS AND METHODS

Morphological studies

Albino Wistar strain male rats (100–150 gm) were anaesthesized with ether and the abdominal cavity opened. The aorta and cava were cut above the liver in order to kill the animal by exsanguination. The thoracic cavity was then exposed without delay, and the left lung was cut out and fixed in 10% formaldehyde. Routine 5 μ-thick haematoxylin and eosin sections were prepared for light microscopy.

To study the perivascular vessels a cannula was introduced in the aorta through the left ventricle, and the vessels were first washed with a saline solution. Next, the aorta was tied just above the diaphragm and India ink injected into the vessels. The left lung was fixed in 10% formaldehyde and portions were processed for paraffin sections stained with haematoxylin and eosin as well as for 30 μ-thick frozen unstained preparations mounted in glycerin jelly.

For electron microscopic observations the same procedure was followed until exposure of the lungs. The left lung was then cut out and immersed in 2.5% glutaraldehyde buffered with 0.1 M phosphate and maintained at 4°C. Fixation by injection of fixative through the trachea or by perfusion through the pulmonary artery under controlled pressure was tried but with no advantage over the method of immersion. A slice as thin as possible was cut with a razor blade under fixative and then minced. The tissue was further fixed with glutaraldehyde, post-fixed with osmium tetroxide and embedded in araldite (Cargille). Thin sections cut with glass or diamond knives by means of a Porter-Blum MT-2 microtome were mounted on 300-mesh copper grids and stained with uranyl acetate and lead citrate. Sections were examined with an AEI-EM6B electron microscope.

Electrophysiological studies

Albino rats were killed with a blow on the head and the lungs were quickly excised and immersed in Tyrode solution (NaCl, 137 mM; KCl, 2.7 mM; $CaCl_2$, 2.5 mM; $NaHCO_3$, 12 mM; NaH_2PO_4, 1.8 mM; $MgCl_2$, 0.6 mM; dextrose, 6 mM) equilibrated with a 95% O_2 – 5% CO_2 gas mixture at ambient pressure and temperature. A preparation containing lungs, pulmonary veins and most of the left atrium was dissected and pinned to a paraffin bed under a constant flow of Tyrode solution at 37°C. The lungs were trimmed down to their juxtahilar portions as no great mass of tissue is adequately supplied with oxygen by the present method. Preparations were electrically stimulated through a pair of stainless steel needles pinned to the left atrial roof. Stimuli were rectangular 2-millisecond-long pulses of 1.5–2 × threshold intensity, isolated from earth by means of a Bioelectric Instruments ISA-100 unit. Transmembrane recording was obtained through 3M KCl-filled glass microelectrodes, with a DC resistance of 20–30 M. Potentials were measured with respect to a bath ground with the aid of a neutralized input capacitance preamplifier (Bioelectric Instruments, NF-1). A 565 Tektronix double beam oscilloscope was used to display transmembrane potentials either as a function of time or against their first time derivative, obtained through a Tektronix type O operational amplifier. Calibration of both types of records were obtained by applying between bath and ground a rectangular pulse of known duration and voltage, or a ramp of known slope and amplitude. Permanent records of the oscilloscope display were taken on film with the aid of a Grass C–4 camera.

The effect of acetylcholine (ACh) on transmembrane recordings was studied by local extracellular application of a 30 μg/ml solution of acetylcholine hydrochloride (Roche) in Tyrode. The application of ACh

was made with the aid of a 50–70 μ-thick glass micropipette connected to a glass syringe.

RESULTS

Structure of the pulmonary vein

There is no general agreement regarding the components of vein wall. Policard et al. ('59) considered the true wall of the vein to be composed of endothelium and smooth muscle layers. We include the striated muscular coat as part of the venous architecture and recognize: (1) an endothelial layer; (2) a subendothelial layer; (3) an internal connective tissue layer; (4) a striated muscle layer and (5) an external connective tissue layer (figs. 1, 2, 8).

The subendothelial layer is composed of smooth muscle fibers which can be traced into lung venules as small as 25 μ in diameter. This layer (1 to 5 cells thick) does not increase proportionally to the lumen. In the larger veins at the hilum, whose diameter measures 400–600 μ and whose wall is 85 μ thick, there is sometimes only a sheath one fiber thick beneath the endothelium. Electron microscopy reveals this single layer to be discontinuous. When smooth muscle is absent, the endothelium is only separated from the striated muscle layer by the internal connective tissue (figs. 2, 7, 8). On the other hand, in smaller veins, 50–200 μ, the smooth muscle cells accumulate and form small cushions that push the endothelium toward the lumen (fig. 3). The smooth muscle fibers are generally close to each other and embedded in a matrix containing collagen fibrils and elastic lamellae. The amorphous matrix is scanty between their membranes and those of the endothelium and they seem to adhere to each other (fig. 8).

The internal connective tissue layer is composed of a dense matrix substance, fibroblasts, collagen fibrils and elastic lamellae. The width of this layer varies from 1–6 μ but part of the thickness may be due to artifacts (figs. 7, 8).

The striated muscle layer is continuous with the myocardium of the left atrium. At the great vein of the left pulmonary hilum it may be eight cells thick but the variations are too great to establish an average. According to our experience these fibers form an external coat with a longitudinal orientation and an internal circular bundle, both approximately of the same thickness (fig. 2). As the diameter of the veins diminishes the striated muscle layer gradually tapers off, constituting only a one-cell-thick sleeve in vessels measuring 130–150 μ. It disappears completely when the veins attain about 100 μ diameter. The external longitudinal bundle extends further in the lung than the circular one, as illustrated in figure 1. Small secondary branches of the main pulmonary vein about 60 μ in diameter do not have striated muscle (fig. 4).

India ink injections display a rich net of vasa vasorum in this muscle layer (fig. 5). It seems that along each muscle fiber runs one capillary following the orientation of the fiber (fig. 6). The larger vessels have diameters of 20–30 μ, and the smallest 3–6 μ. No vasa vasorum were found in the subendothelial layer or in the pulmonary arteries inside the lung.

The external connective tissue forms a large perivascular space and has a loose matrix substance with collagen, fibroblasts, leucocytes and many vessels, mainly lymphatics (figs. 1, 4).

The above-mentioned figures are typical values and it must be remembered that there are great variations from animal to animal. For example, in one case the striated muscle layer vanished from the pulmonary vein at the hilum when the vessels measured 300 μ in diameter.

Ultrastructural features of the striated muscle layer

The striated muscle layer is constituted of muscle cells of cardiac type with one, rarely two, centrally located nuclei, and containing a great number of mitochondria and glycogen granules. The diameter of each fiber varies from 8–20 μ and that of the fibrils from 0.6–1.2 μ (figs. 9, 10). Generally they are contracted or semicontracted and relaxed fibers are difficult to observe. Thus, the sarcomere measured 1.2–1.5 μ when contracted and 2.1 μ in the most relaxed fibril.

Other measurements are: A band = 1.2–1.4 μ; I band (not always present) = 0.2–0.6 μ; H band (constituted almost exclusively by the M band) = 60–90 mμ; Z line = 50–100 mμ; primary myofilament (diameter) = 16 mμ; secondary myofilaments (diameter) = 5 mμ (figs. 11a,b).

The transverse sections of the filaments strongly suggest a hexagonal array but for some reason we could not get the clear image observed in other striated muscles. The primary myofilaments look in cross sections rather like tubules than solid structures (fig. 12a).

Great numbers of mitochondria accumulate in the interfibrillar cytoplasm, forming long rows. They are also present in the perinuclear region around the Golgi apparatus and beneath the plasma membrane. The interfibrillar mitochondria are elongated and may attain the length of a sarcomere. One of their extremities, if not both, terminates at a Z band. The mitochondria are of varying width from 0.4–1.0 μ. Their cristae seem randomly oriented. At the periphery of the cell the mitochondria leave a narrow strip of cytoplasm, 50–100 mμ wide, between themselves and the sarcolemma but sometimes at cell interconnections their membranes are very close to the plasma membrane (fig. 15).

The endoplasmic reticulum, subsurface vesicles, sarcotubular system, sarcolemma and basement membrane seem the same as described by Karrer ('59; '60) in mice (fig. 12).

Intercalated discs were observed by light and electron microscopy (figs. 13, 14, 15). This old term is fine for the thick transverse bands seen in light microscopy but we prefer to use the term intercellular junction for the ultrastructural description of this feature (DISCUSSION). The intercellular junctions are oriented transversely and longitudinally. The transverse interconnections are step-like with both transverse and longitudinal segments. The transverse segment of the transverse interconnection has a wavy pattern and generally is of the length of one or two sarcomeres (fig. 13). Continuous with the transverse interconnection there are lateral interconnections which most frequently have the same length as a sarcomere (fig. 14). Within the intercellular junctions the three types of junctional specializations (McNutt, '70) may be observed (figs. 13, 15). The fasciae adherentes occupy almost completely the transverse segments of the transverse interconnections and seem to be in the place of Z bands. They are surrounded by a condensed filamentous material in which enter the myofilaments. The maculae adherentes (desmosomes) are frequently observed in both lateral and transverse interconnections. They are also surrounded by condensed filamentous material but next to it there is an electron-transparent halo suggesting the absence of insertion of myofilaments. The intercellular gaps in the fasciae and maculae adherentes measure about 20 mμ. The nexuses (tight junctions, gap junctions, pentalaminar junctions, quintuple-layered interconnections) are either in the longitudinal interconnections or in the longitudinal segments of the transverse interconnections. We saw them as trilaminar and as pentalaminar structures (fig. 15).

Nerve fibers with nonmyelinated axons surrounded by Schwann cells are common in the striated muscle layer of the pulmonary vein (figs. 16, 17, 18). The diameter of the axons varies from 0.1–1.0 μ and small mitochondria and synaptic vesicles can be observed in their axoplasm. Axons containing small vesicles with electron-dense cores suggestive of adrenergic innervation can be seen. Nerve endings with many small electron-translucent vesicles and some larger vesicles with dark granules characteristic of cholinergic innervation are also present, although they are difficult to find (figs. 16, 19). We did not observe any contact of the axolemma with the sarcolemma; there was always a gap of 0.2–0.4 μ between these structures. There are no specializations of the muscle cell membrane in the proximity of the axon terminals (fig. 19).

There are many vessels in the striated muscle layer and the capillaries are very close to the muscle cells, leaving a narrow band of interstitium measuring about 150–200 mμ (figs. 20, 21). The capillary walls are one or two endothelial cells in thickness. The cytoplasmic ends of these cells are united by tight junctions, sometimes very long and sinuous. In the inner border of these junctions a small cytoplasmic tongue projecting toward the lumen may be observed (fig. 21). Besides the mitochondria, endoplasmic reticulum and Golgi apparatus there is an impressive number of pynocytotic vesicles in the endothelium of the capillaries. Pseudofenestrations are rarely present in the walls of

these vessels. They measure about 100 mμ and apparently are bridged by a membrane formed by endothelial cells. In these sites the basement membrane does not suffer any interruption (fig. 21).

Propagation of excitation in pulmonary veins

Twenty isolated left atrium-pulmonary vein preparations were used in this study. They were mostly quiescent, or could be made so by trimming off attached bits of right atrium. All preparations responded to electrical stimulation of the left atrial roof (1/sec) with a propagated action potential which invaded the walls of all pulmonary veins and traveled toward the lungs. The microelectrodes had access only to the extrapulmonary segment of the veins.

Figure 22 shows a drawing of one of the preparations. Each figure represents time in milliseconds between stimulus and the arrival of activity (upstroke of action potential) at that point. Propagation velocity in pulmonary venous tissue could then be calculated from timing and from the location of the recording site as given by a rectangular coordinate vernier system adapted to the micromanipulator that carried the electrode. Measurements obtained from seven preparations, where 66 cell impalements were made, yielded values of 0.5–1.2 m/sec.

Action potential shapes in pulmonary veins resembled those obtained from left atrium (fig. 23A). The phase plane display indicated that the upstroke of these potentials is a simple S-shaped waveform with a maximum rate of depolarization ranging from 200–600 volts/sec. These fast upstrokes are suggestive of a strong, Na-dependent fast component. No slow-rising, nodal-like action potentials were observed in any of the 227 cell impalements performed throughout the preparations.

However, several preparations developed short or prolonged trains of tachycardia which could be overcome by further atrial trimming or an increase in the rate of stimulation.

Effect of acetylcholine (ACh) on pulmonary vein electrical activity

ACh applied directly to the site of recording by means of a micropipette caused a decrease in the duration of the action potentials of both left atrium and pulmonary vein (fig. 23A,B). A modest degree of hyperpolarization was present in both cases. The peak voltage and maximum rate of rise of the upstroke was not altered by ACh in either case.

DISCUSSION

The morphology of the pulmonary vasculature has been generally accepted as appropriate to the periods of high and low resistance characteristically observed in the return of blood to the left atrium. It was thought that the veins of the lung were able to distend and that their capacity for constriction was rather low. This view has been challenged and it has been shown that vasoconstriction does occur in the pulmonary veins under special conditions (Hyman, '66). The presence of a conspicuous striated muscle layer resembling cardiac muscle in the pulmonary veins of some animals indicates that these vessels may play a hitherto unknown role in the circulation and that they may exhibit a dynamic behavior during the cardiac cycle. The rat is a convenient animal for the study of this phenomenon because the striated muscle layer of its pulmonary vein is easily observable and extends deeply into the lung. Considering that in previous papers rodents were also studied, our morphological observations in the Wistar rat are surprising. Karrer ('59, '60) and Heppleston ('61) worked with mice, Ludatscher ('68) with Buffalo rats. Policard et al. ('59) also worked with rats but do not mention the species. The differences noted here and by these workers are not only in ultrastructural details but in the general aspects of the venous structure.

The striated muscle layer in the mouse extends to the smallest branches of the pulmonary veins but Karrer (op. cit.) could not distinguish separate circular and longitudinal bundles in his material. Moreover, smooth muscle cells are completely absent from the vessel wall in these animals.

The Buffalo rat has striated muscle cells in the wall of veins down to the size of 20–30 μ; and the internal subendothelial layer of smooth muscle, which occurs in the smallest ramifications of the pulmo-

nary veins, increases proportionally to the lumen of the vessels (Ludatscher, '68).

The striated muscle layer in the pulmonary veins of the Wistar rat can be found in vessels as small as 100 μ in diameter. In this respect they are similar to the species of rat (*Mus decumanus*) observed by Granel ('21) with the light microscope.

The subendothelial layer of smooth muscle cells in the Wistar rat is irregular. First, in the larger pulmonary veins it is not continuous and it is because of this histological peculiarity that we prefer to consider the striated muscle layer as part of the venous wall and not of an external sleeve as regarded by some authors (Policard et al., '59). Next, there are small cushions in the medium-sized veins, which were not reported by other researchers.

Policard et al. do not mention the length of extension of the striated muscle along pulmonary veins nor do they give details about the subendothelial layer. But the size they reported for myofibrils (0.2–0.4 μ) and sarcomeres (0.3–0.4 μ) is considerably less than in the mouse and Wistar rat (0.6–1.2 μ for fibrils and 1.2–2.1 μ for sarcomeres). This is a rather puzzling difference, especially considering that their measurements for mitochondria and myofilaments are roughly the same as ours and therefore their findings cannot be explained by preparation artifacts.

Our ultrastructural details approach very much Karrer's findings in the mouse. There is one aspect worthy of comment: he did not find typical M bands and the I bands were either narrow or indistinct. Although this was ascribed to the states of contraction of the muscle fibers, Karrer suggested that the narrow I bands could perhaps be responsible for a smaller contractile power which would be, of course, an important feature for pulmonary haemodynamics. We had no difficulty in finding M or I bands. Judging by standards of rat heart I bands (Muir, '57; Stenger and Spiro, '61), we do not think that there are morphological reasons to postulate a diminished contractile power.

As did Karrer, we found that the myofilaments are not as regularly arranged as in other striated muscles. We were impressed by the difficulty in getting a good view of the cross section of the myofilaments. The hexagonal array of the filaments was rarely seen but it does exist. The primary myofilaments often seemed hollow, as would be the appearance of a tubular structure (fig. 12a). We have no explanation for this finding.

The intercalated disc or intercellular junctions of the striated muscle of the pulmonary vein look like those of the heart, as recently reviewed by McNutt ('70). We believe that certain discrepancies between observations on pulmonary veins and the heart are due rather to conceptual than to structural differences. As McNutt remarked, there are authors who use the term intercalated disc in electron microscopy to describe only the transverse segment of the transverse interconnections whereas this denomination should be applied to the entire transverse interconnection with its transverse and longitudinal segments. The heptalaminar nexus was not seen by us because all our blocks were stained by uranyl acetate and lead citrate, a treatment which prevents the visualization of this seven-layered ultrastructure.

There has been much discussion about the innervation of the pulmonary vessels. It is generally agreed that the pulmonary veins are supplied by the cardiac and pulmonary plexuses and that histochemical techniques show adrenergic and cholinergic nerves in the larger pulmonary veins of rat (Fisher, '65; Cech, '69; El-Bermani et al., '70). We did not find any specialized myoneuronal junction in the pulmonary vein nor did we register any nerve endings as close to the muscle cell as Karrer ('59) shows in his figure 11. Direct termination of axons on the cell membrane was rarely seen in the heart muscle (Viragh and Porte, '61; Thaemert, '66). Generally there is a gap wider than 100 mμ between both structure. Morphologically our observations are almost identical to those of Iwayama et al. ('70) on the innervation of the cerebral arteries of the rat, which they described as possessing adrenergic and cholinergic nerve endings and lacking specialized myoneuronal junctions.

The presence of pseudo-fenestrations in the capillaries of the striated muscle layer deserves comment. We do not think that the structure of these thin regions is an artifact because the material seems well preserved and Karrer ('60) found similar

structures in the mouse. There they were 65 mμ in size and were called pores. In our experience they may be larger (100 mμ) and differ from true fenestrations by having a distinct membrane. Pietra et al. ('71) administered histamine to dogs and using colloidal carbon as an electron-dense tracer observed that the first vessels to leak carbon were the bronchial venules. They saw endothelial gaps approximately 100–500 mμ wide. In view of these findings it is admissible that the pseudo-fenestrations in the capillaries of the pulmonary vein may play an important role in the development of the perivascular interstitial edema that appears so early in pulmonary edemas.

The electrophysiological data fully support the notion that the striated muscle layer of pulmonary veins in the rat is indeed similar to and functionally connected with the left atrial myocardium, at least in their extrapulmonary segment. Their action potential shape, conduction velocity and sensitivity to ACh are indistinguishable from those of atria (Hoffman and Cranefield, '60). Such findings are in general agreement with those of MacLeod and Hunter ('67) who studied strips of rat atria and thoracic veins. It seems worthwhile pointing out, however, that we could not confirm their observation of a decrease in action potential amplitude after treatment with ACh. The discrepancy may be due to the poor frequency response of their mechanical recorder and consequent loss of amplitude in the recording of the very fast and short wave forms obtained with ACh. We did not obtain any evidence of a slow, ACh-sensitive phase in the upstroke of the action potential of rat atrial or pulmonary vein myocardium, as can be seen in the phase-plane records with control or ACh solutions. Comparison with results obtained from rabbit atria (Paes de Carvalho et al., '69) suggest that both atrial and pulmonary venous myocardial cells of the rat exhibit a fully developed and activated fast component.

The question now arises as to the physiological way in which the rat's pulmonary vein myocardium is excited. Left atrium is normally excited by propagation from a right atrial pacemaker, the sinus node or its venous wall equivalent (Paes de Carvalho et al., '59). Activation of the rat's left atrium was shown here to propagate up the pulmonary veins toward the lungs. No propagation difficulty or slow nodal-like region could be detected between left atrium and pulmonary veins in this study. The occurrence of nexuses between myocardial cells in the venous wall support the idea of a simple cell-to-cell propagation. It is therefore justifiable to state that pulmonary vein myocardium beats in response to a propagation wave that travels *toward* the lung. Any possible physiological "milking" action of the vein in favor of blood return toward left atrium can thus be discarded. The results of Spach et al. ('72), who studied electrical propagation in the thoracic veins of infants and dogs, support this view. On the other hand, the practical importance of arrhythmias restricted to or originating in these veins remains to be determined in the light of better understanding of pulmonary vein mechanics and haemodynamics.

Some speculative ideas have been put forth by several authors as to the function of muscle in the pulmonary veins. In 1877 Arnstein (cit. in Karrer, '59) assumed that the striated muscle sleeve was a functional substitute of the venous valves. A similar idea was advanced by Burch and Romney ('54) who studied veins of five human hearts and proposed for them a "throttle valve" action to prevent the backflow of blood during atrial systole. Our results are compatible with these ideas in that a quasi-simultaneous contraction of left atrium and pulmonary veins would effectively augment resistance to backflow of blood into the lung without preventing the normal flow pattern during diastole. In this sense, weakening or mechanical insufficiency of the myocardial coat of pulmonary veins could be instrumental in increasing pressure in lung capillaries and favoring edema. If any such mechanism exists it should be more important in rat and mouse than in man and dog. The lung of the rat is very much predisposed to congestion and haemorrhage (Böhm et al., '72). Even to obtain normal rat lung is difficult; the methods of sacrifice provoke pulmonary haemorrhages. That is the reason why we kill these animals by exsanguination.

Considering the extension of the cardiac muscle layer along the pulmonary veins

one should speculate that alterations in the capacitance of these vessels occur. However, as pointed out by Spach et al. ('72), one should keep in mind that the extension of cardiac muscle toward thoracic veins is prominent in the embryo and recedes progressively after birth. Congenital anomalies involving persistence of these structures can thus occur and might conceivably result in circulatory disturbances.

It should also be pointed out that cardiac muscle is incapable of strong maintained contracture, even though its resting tension can vary with distension as well as with some physiological and pathological situations. On the other hand the smooth muscle layer, incomplete as it may be, can be expected to respond with changes in tone to different neurohumoral and pharmacological agents. Effects of this sort seem to constitute a more likely explanation for results such as those of Eliakim and Aviado ('61) who found that different agents affected the resistance of pulmonary veins in a tonic manner. The venous smooth muscle layer should be taken into consideration separately when dealing with the pathophysiology of pulmonary blood return to the heart.

LITERATURE CITED

Best, P. V., and D. Heath 1961 Interpretation of the appearances of the small pulmonary blood vessels in animals. Circ. Res., *9:* 288–294.

Böhm, G. M., I. Vugman, V. Valeri, W. Sarti, I. F. Carvalho and J. A. Laus Filho 1973 Ultrastructural alterations to pulmonary blood vessels in acute immunological lung lesion in rats, mice and guinea-pigs. J. Path., *111:* 95–101.

Burch, G. E., and R. B. Romney 1954 Functional anatomy and "throttle valve" action of the pulmonary veins. Amer. Heart J., *47:* 58–66.

Cech, S. 1969 Adrenergic innervation of blood vessels in the lung of some mammals. Acta Anat., *74:* 169–182.

El-Bermani, A. W., W. F. Mcnary and D. E. Bradley 1970 The distribution of acetylcholinesterase and catecholamine containing nerves in the rat lung. Anat. Rec., *167:* 205–212.

Eliakim, M., and D. M. Aviado 1961 Effects of nerve stimulation and drugs on the extrapulmonary portion of the pulmonary vein. J. Pharm. Exp. Ther., *133:* 304–312.

Favaro, G. 1910 Il miocardio polmonaire. Contributi all'isotologia umana e comparata dei vasipolmonari. Internat. Monatschr. Anat. Physiol., *27:* 376–401.

Fisher, A. W. J. 1965 The intrinsic innervation of the pulmonary vessels. Acta Anat., *60:* 481–496.

Granel, F. 1921 Sur la musculature striée des veines pulmonaires du rat. C. R. Soc. Biol., *84:* 291–294.

Guieysse-Pellisier, A. 1945 Les Appareils Respiratoires dans la Série Animale. Payot, Paris, pp. 233–235.

Heppleston, A. C. 1961 The musculature of the aging mouse lung. A light and electron microscope study. J. Gerontology., *16:* 106–109.

Hoffman, B. F., and P. E. Cranefield 1960 Electrophysiology of the Heart. McGraw-Hill Book Co., New York.

Hyman, A. L. 1966 The pulmonary veins. Ann. Rev. Med., *17:* 431–446.

Iwayama, T., J. B. Furness and G. Burnstock 1970 Dual adrenergic and cholinergic innervation of the central arteries of the rat. Circ. Res., *18:* 635–646.

Karrer, H. E. 1959 The striated musculature of blood vessels. I. General cell morphology. J. Biophysic. Biochem. Cytol., *6:* 383–392.

——— 1960 The striated musculature of blood vessels. II. Cell interconnections and cell surface. J. Biophys. Biochem. Cytol., *8:* 135–150.

Klavins, J. V. 1963 Demonstration of striated muscle in the pulmonary vein of the rat. J. Anat. London., *97:* 239–241.

Kramer, A. W., Jr., and L. S. Marks 1965 The occurrence of cardiac muscle in the pulmonary veins of Rodentia. J. Morph., *117:* 135–150.

Ludatscher, R. M. 1968 Fine structure of the muscular wall of rat pulmonary veins. J. Anat., *103:* 345–357.

MacLeod, D. P., and E. G. Hunter 1967 The pharmacology of the cardiac muscle of the great veins of the rat. Canad. J. Physiol. Pharm., *45:* 463–473.

McNutt, N. S. 1970 Ultrastructure of intercellular junctions in adult and developing cardiac muscle. Amer. J. Cardiol., *25:* 169–183.

Muir, A. R. 1957 An electron microscope study of the embryology of the intercalated disc in the heart of the rabbit. J. Biophysic and Biochem Cytol., *3:* 193–202.

Nathan, H., and H. Gloobe 1970 Myocardial atrio-venous junctions and extensions (sleeves) over the pulmonary and caval veins. Thorax, *25:* 317–324.

Paes de Carvalho, A., W. C. Mello and B. F. Hoffman 1959 Electrophysiological evidence for specialized fiber types in rabbit atrium. Amer. J. Physiol., *196:* 483–488.

Paes de Carvalho, A., B. F. Hoffman and M. Paula Carvalho 1969 Two components of the cardiac action potential. I. Voltage-time course and the effect of acetylcholine on atrial and nodal cells of the rabbit heart. J. Gen. Physiol., *54:* 607–635.

Pietra, G. G., J. P. Szidon, M. M. Leventhal and A. P. Fishamn 1971 Histamine and interstitial pulmonary edema in the dog. Circ. Res., *29:* 323–337.

Policard, A., A. Collet and S. Prégermain 1959 La gaine myocardique des veines intrapulmonaires étudiee chez le rat au microscope electronique. Bull. Micr. Appl., *9:* 5–9.

Spach, S. M., C. B. Roger and P. H. Jewtt 1972 Spread of excitation from the atrium into thoracic veins in human beings and dogs. Amer. J. Cardiol., *30:* 844–854.

Stenger, R. J., and D. Spiro 1961 The ultrastructure of mammalian cardiac muscle. J. Biophys. Biochem. Cyt., *9*: 325–352.

Stiede, L. 1877 Ueber quergestreifte Muskelfasern in der Wand der Lungenvenen. Arch. Mikr. Anat., *14*: 243–248.

Thaemert, J. C. 1966 Ultrastructure of cardiac and nerve contiguities. J. Cell Biol., *29*: 156–162.

Virágh, S., and A. Porte 1961 Elements nerveux intracardiaques et innervation du myocarde. Étude au microscope électronique dans le coeur de rat. Z. Zellforsch., 55: 282–296.

PLATE 1

EXPLANATION OF FIGURES

1 Main branch of the left pulmonary vein of a Wistar rat. External connective tissue layer (ec); striated muscle layer (*mc*). The arrow is indicating a longitudinally oriented muscle fiber. Five micron section; haematoxylin and eosin. × 72.

2 Wall of the left pulmonary vein. Internal circular (ci) and external longitudinal (lo) bundles of striated muscle layer. The endothelium (en) is covered with carbon particles and some smooth muscle cells may be observed beneath it. Five micron section; haematoxylin and eosin. × 400.

3 Small pulmonary vein (65 μ diameter). There is no striated muscle layer; the smooth muscle cells (sm) form cushions that push the endothelium toward the lumen. The star is on a clump of carbon particles. Five micron section; haematoxylin and eosin. × 400.

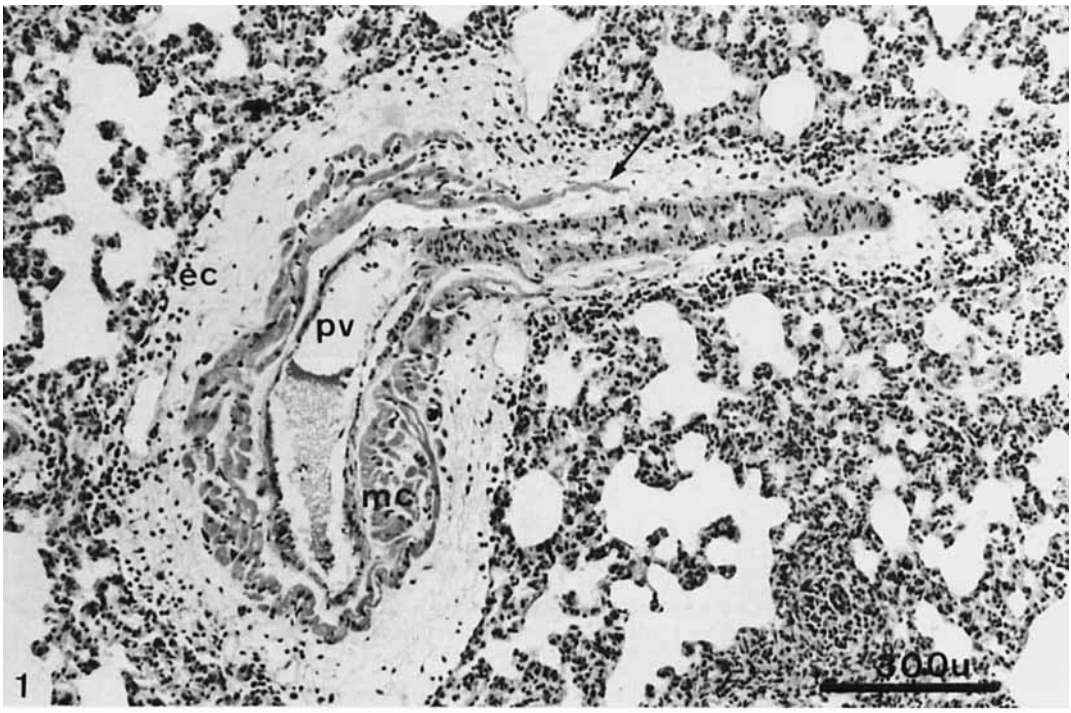
ec
pv
mc
1
600u

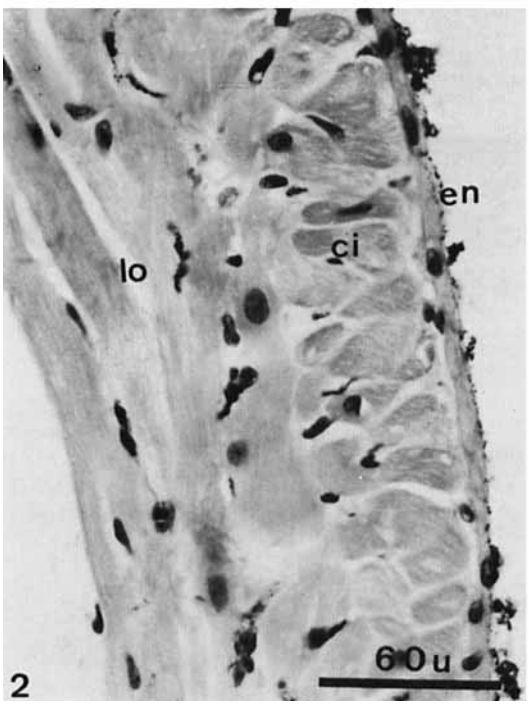
en
ci
lo
2
60u

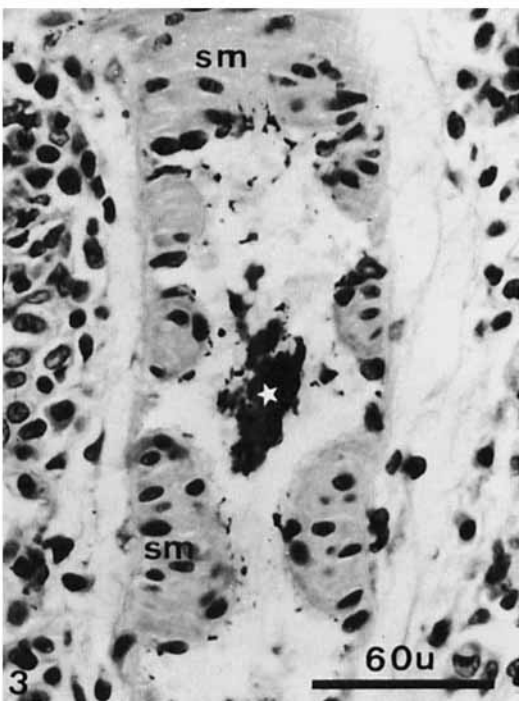
sm
sm
3
60u

PLATE 2

EXPLANATION OF FIGURES

4 Left pulmonary vein. The arrow is showing a secondary branch (60 μ diameter) without striated muscle layer (mc). *b*, main left bronchus. Five micron section; haematoxylin and eosin. × 72.

5 Wall of the left pulmonary vein showing the vasa vasorum injected with India ink. *en*, endothelium. Ninety micron-thick frozen, unstained section mounted in glycerin jelly. × 108.

6 Vasa vasorum of the striated muscle layer of the left pulmonary vein. There is a capillary (c) between each muscle cell. *d*, intercalated disc of the striated fibers. Five micron section; haematoxylin and eosin. × 540.

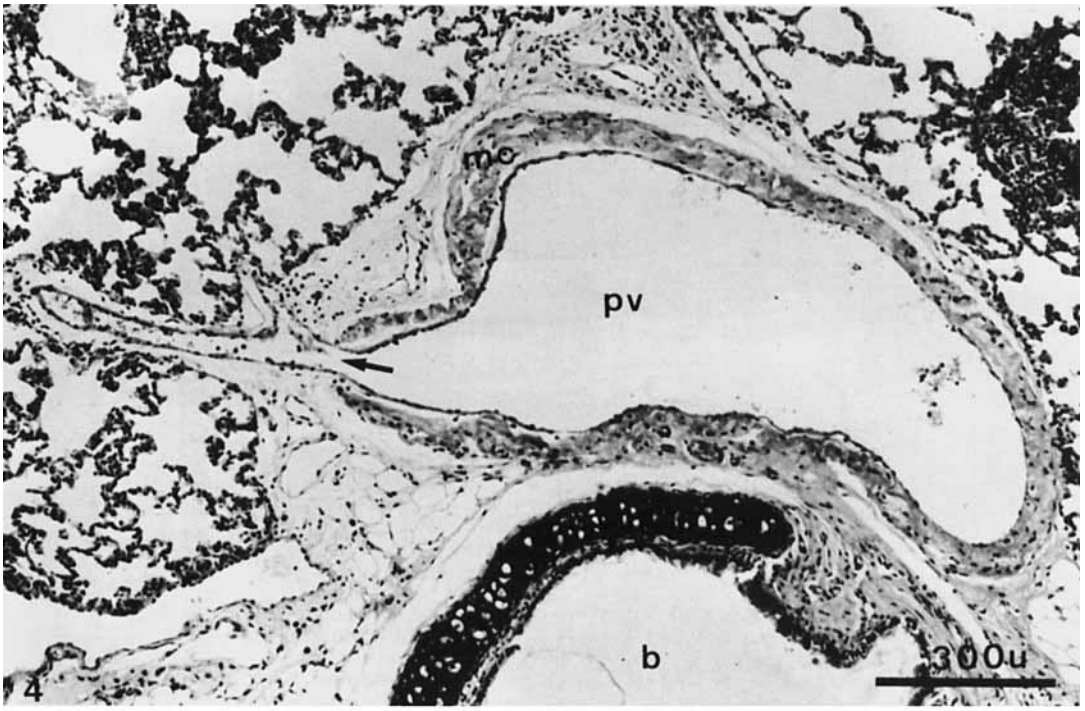
mc
pv
b
300u
4


en
200u
5

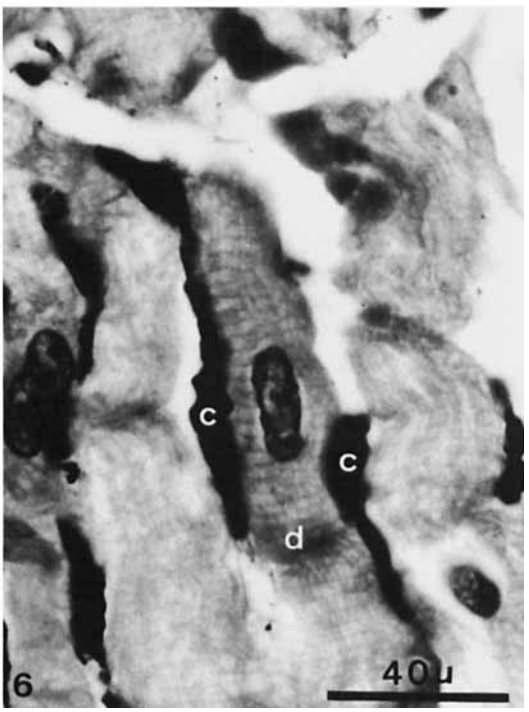
c
c
d
40u
6

PLATE 3

EXPLANATION OF FIGURES

7 Electron micrograph of the pulmonary vein, showing endothelium (en), internal connective tissue layer (ic), and striated muscle layer (mc). At the right side there is an endothelium cell and at left a smooth muscle cell (sm). The smooth muscle fibers do not form a continuous layer beneath the endothelium. This is also clearly shown in figure 7a where there is endothelium (en), internal connective tissue layer with collagen fibrils and striated muscle layer (mc) but no smooth muscle. Figure 7, × 14,400; figure 7a, × 8,800.

8 Electron micrograph of the pulmonary vein. The smooth muscle (sm) is in close contact with the endothelium (en). The internal connective tissue layer (ic) is rich in elastic lamellae. × 14,400.

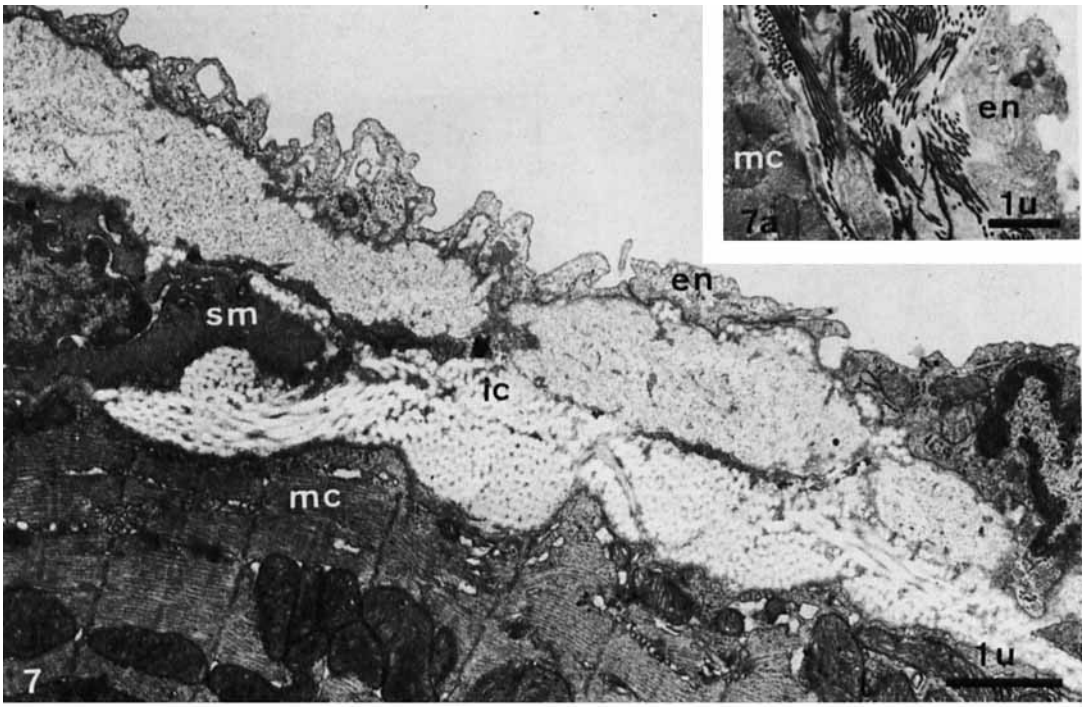
en
mc
7a
1u
en
sm
ic
mc
7
1u

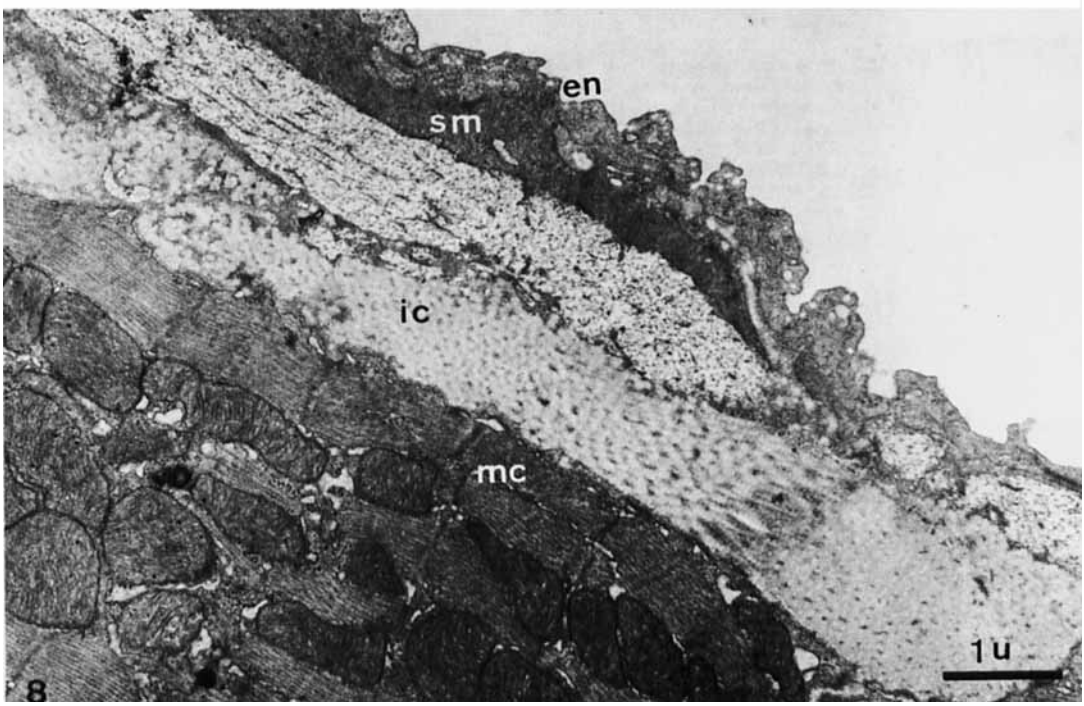
en
sm
ic
mc
1u
8

PLATE 4

EXPLANATION OF FIGURES

9 Electron micrograph of striated muscle fiber. There are two nuclei (n), many mitochondria (mi) and glycogen granules (arrows).

10 Electron micrograph of striated muscle fiber. Between two fibrils (f) there is a row of mitochondria (mi). × 12,400.

11 Electron micrograph of sarcomeres (11a, relaxed fibril; 11b, contracted fibril). The primary and secondary myofilaments are visible. A band (a); H band (h); M band (m); I band (i); Z line (Z). Figures 11a,b, × 34,000.

12 Electron micrograph of the T-system. Interstitial space between two fibers indicated by stars. Long arrows show the sarcolemma and the short arrow points to the basement membrane. Inset, figure 12a, illustrates the transverse section of the myofilaments. The primary filaments look like tubules and occasionally the secondary filaments may be observed in a hexagonal array. Figure 12, × 23,200; figure 12a, × 104,000.

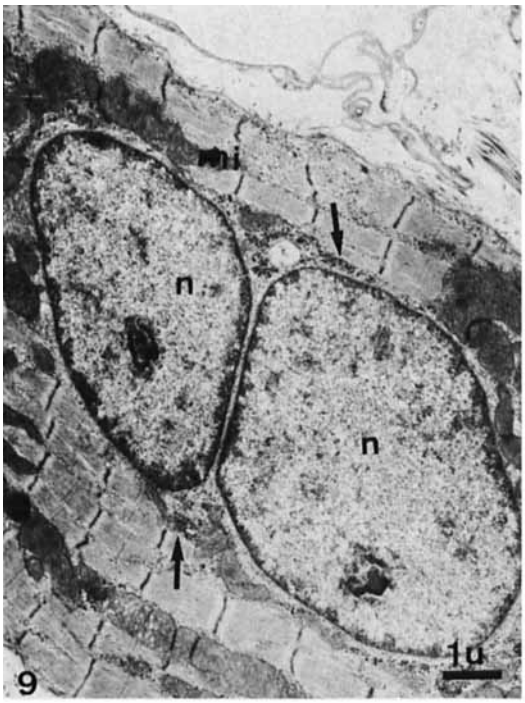
mi
n
n
1u
9


f
mi
1u
10

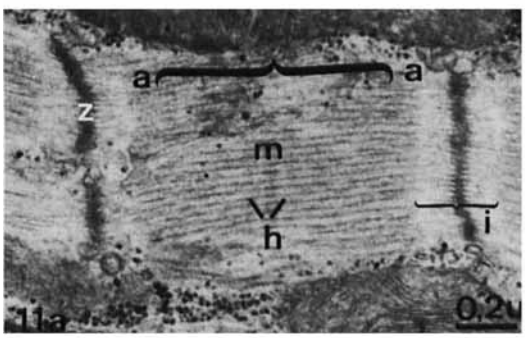
a
a
z
m
h
i
0,2u
11a

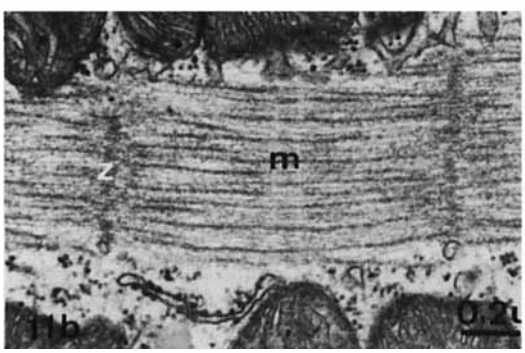
z
m
0,2u
11b

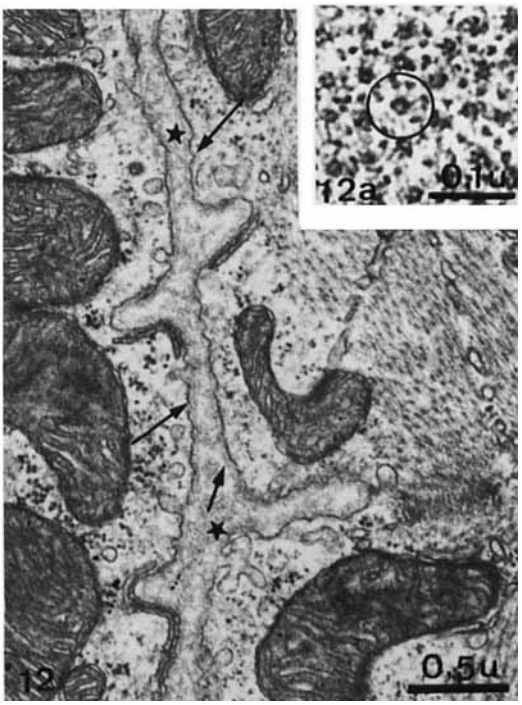
0,5u
12

0,1u
12a

PLATE 5

EXPLANATION OF FIGURES

13 Electron micrograph of a transverse intercellular junction. Transverse segments (t); longitudinal segments (l). Thick arrows show maculae adherentes; straight arrows, fasciae adherentes; curved arrow, nexus. Figure 13a shows the transverse intercellular junction or intercalated disc (d) as it appears with the light microscope. × 17,600.

14 Electron micrograph of intercellular junctions. Beside the transverse junction a longitudinal intercellular junction (lic) may be observed. × 10,400.

15 Electron micrograph of a nexus. The nexus is between two mitochondria (mi) possibly in a longitudinal intercellular junction. In the upper right corner the nexus is enlarged and it is seen as a quintuplelayered structure. Both mitochondria have double membranes, and between them there are three dark lines separated by two clear lines which form the nexus. × 15,600.

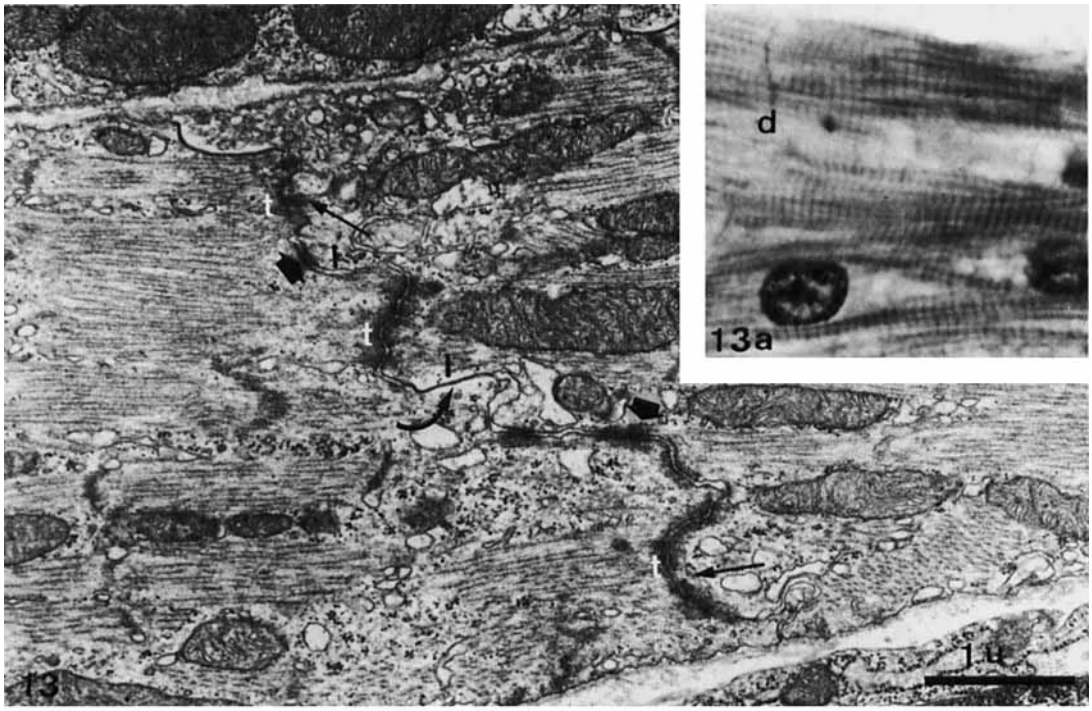
t
l
t
l
t
13
1u

d
13a


lic
14
1u

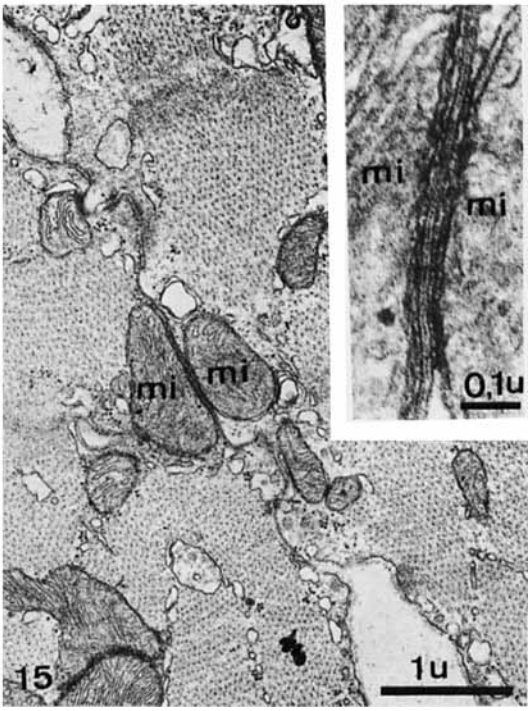
mi
mi
mi
mi
15
1u

mi
mi
0,1u

PLATE 6

EXPLANATION OF FIGURES

16 Electron micrograph of nerve fibers. The presence of small electron-dense vesicles (arrow) suggest that this is an adrenergic nerve ending. × 72,000.

17 Electron micrograph of nerve fibers. The bundle of nerve fibers (arrows) surrounds a capillary with a red cell (r) in its lumen. × 10,400.

18 Electron micrograph of nerve fibers. Although there is a considerable distance between the nerve bundles (n) and the muscle cell (mc) some fibers seem to be nerve endings as they contain typical synaptic vesicles. *c*, capillary. × 10,000.

19 Electron micrograph of a cholinergic nerve ending. The nervous structure contains small translucent vesicles, some larger vesicles with dark granules and mitochondria (mi). The gap between the nerve ending and the muscle cell (mc) measures 0.2–0.4 μ. × 20,800.

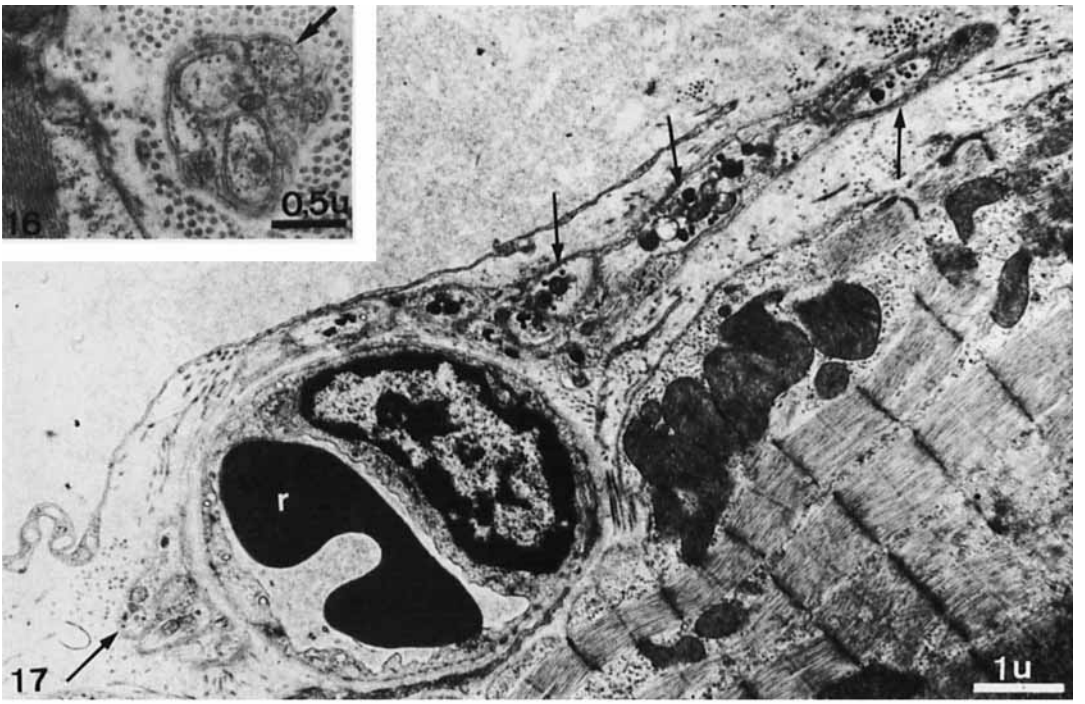
16
0.5u
r
17
1u

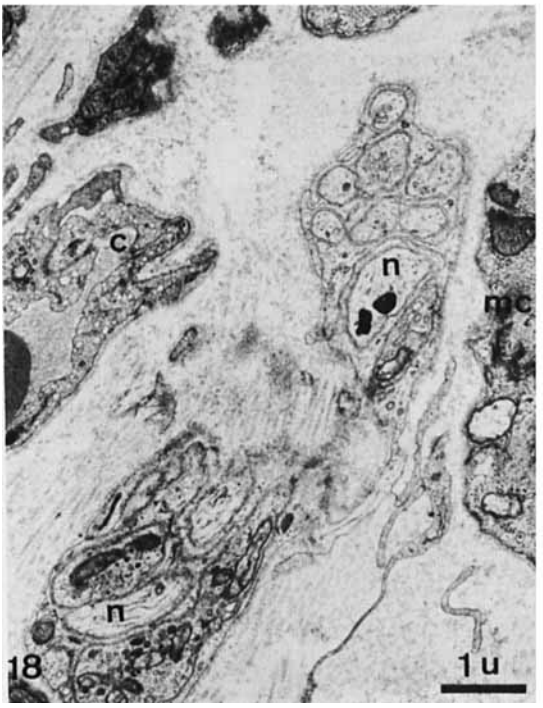
c
n
mc
n
18
1u

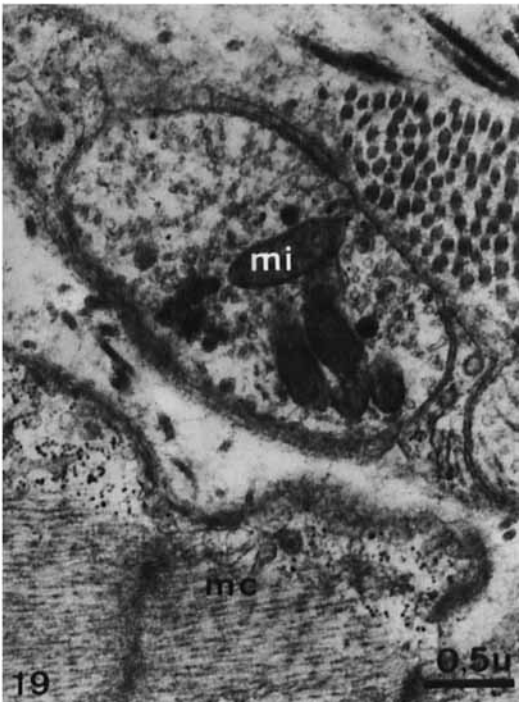
mi
mc
19
0.5u

PLATE 7

EXPLANATION OF FIGURES

20 Electron micrograph of a capillary in the striated muscle layer. The capillary with two red cells (r) in its lumen is very close to the muscle fiber (0.15 μ) and its endothelium contains a great number of pinocytotic vesicles. × 11,200.

21 Electron micrograph of a capillary in the striated muscle layer. Two pseudo-fenestrations (long arrows) may be observed. There is a diaphragm closing the openings and the basement membrane does not suffer interruptions. The endothelial cell junctions are tight and there is a small cytoplasmic process (thick arrow) projecting into the lumen of the capillary. × 16,800.

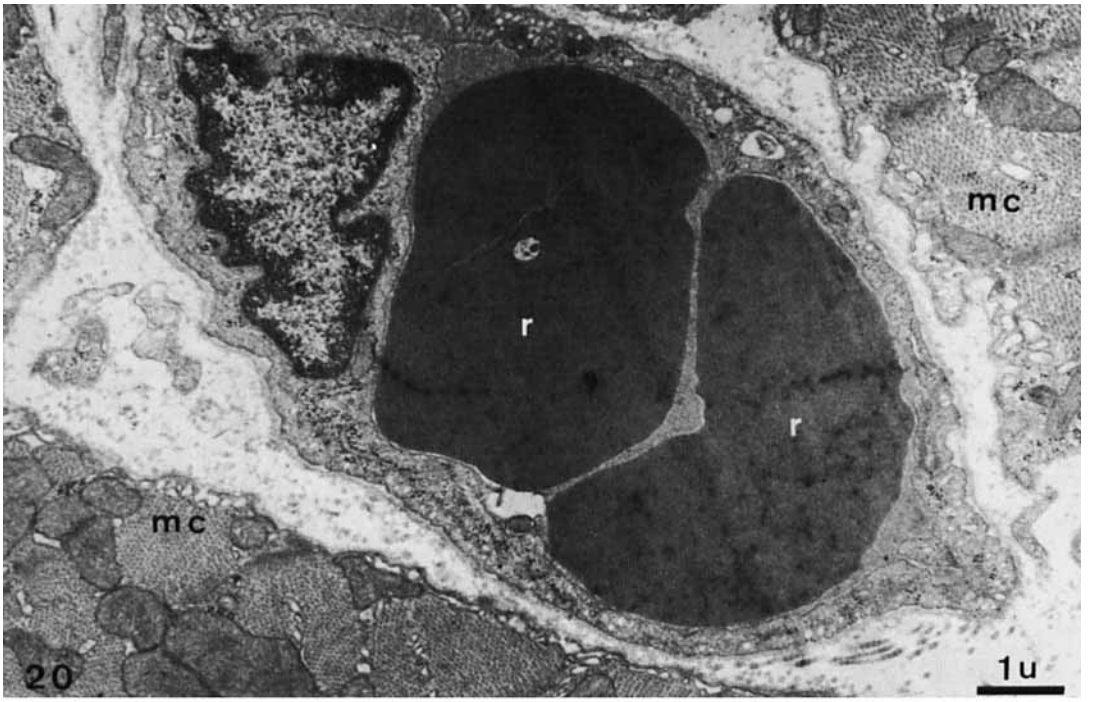
mc
r
r
mc
20
1u

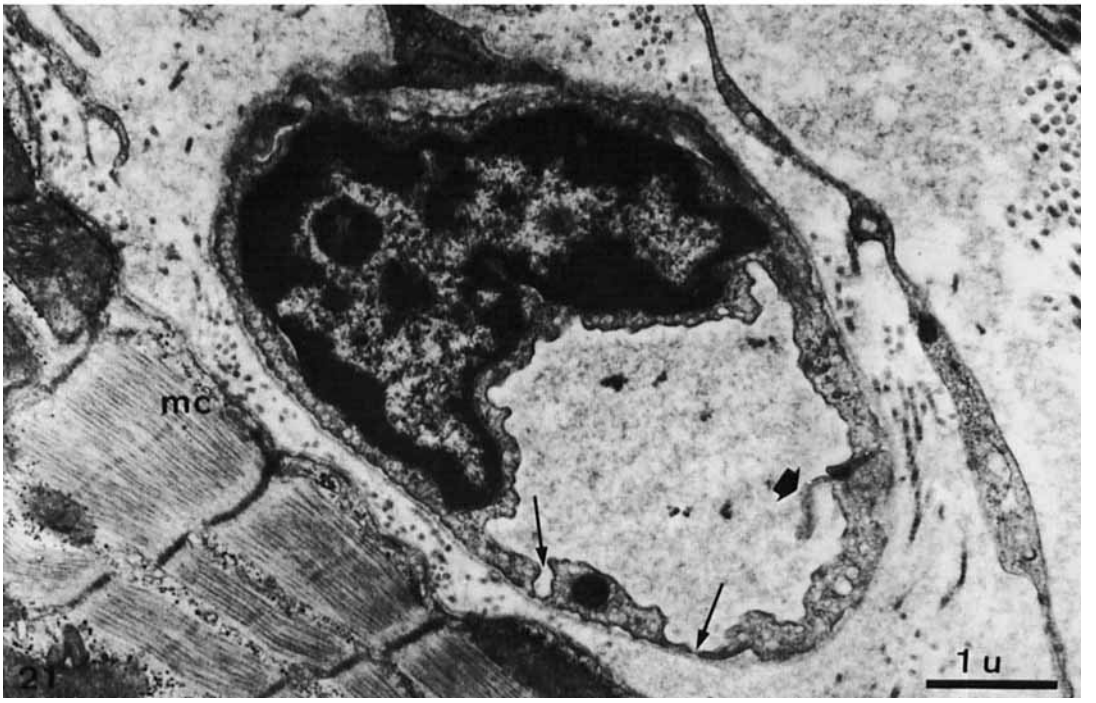
mc
21
1u

PLATE 8

EXPLANATION OF FIGURES

22 Spread of activity along the rat pulmonary veins in a typical preparation. Each figure represents time in milliseconds between stimulus (ST) and arrival of activity at that point. Horizontal and vertical bars = 1 mm.

23 Transmembrane action potential (upper tracing) and phase-plane display (lower right tracing) from the rat pulmonary vein driven from the left atrium. Effect of topical application of acetylcholine. A is record of control in Tyrode solution; B, effect of acetylcholine. Rectangular calibration in upper tracing = 100 mV/10 msec. The plase-plane display shows only the segment corresponding to the upstroke of the action potential and is inscribed from left to right. Vertical bar at lower right corner in each record = V/sec.

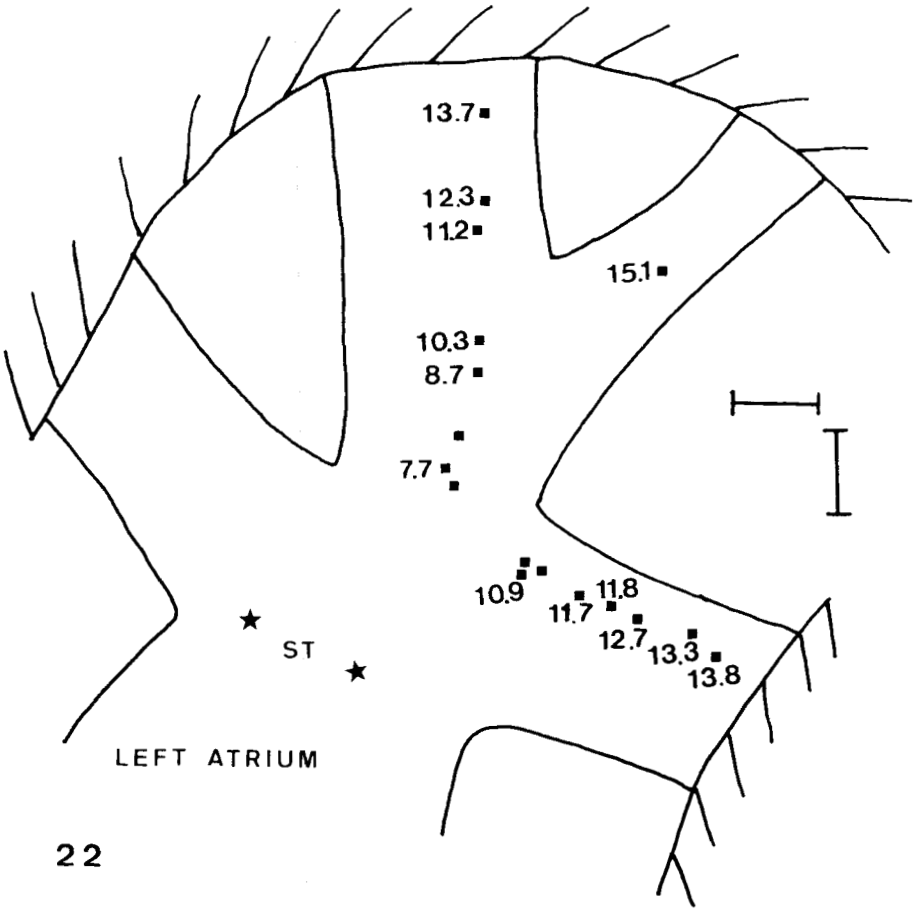
13.7
12.3
11.2
15.1
10.3
8.7
7.7
10.9
11.7
11.8
12.7
13.3
13.8
ST
LEFT ATRIUM

22

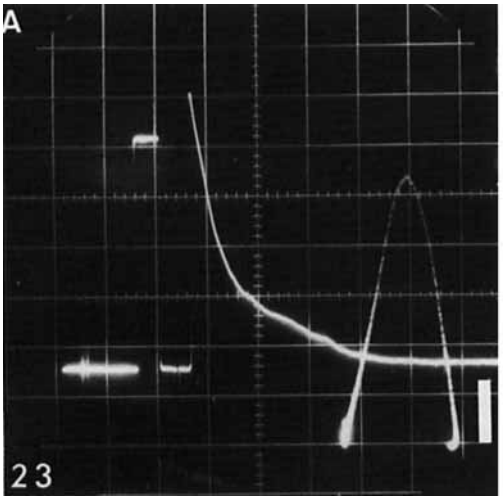
A

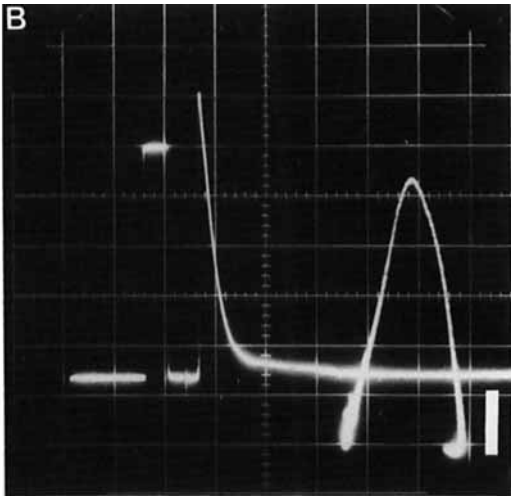
B

23